A Physical Model for Studying Adhesion between a Living Cell and a Spherical Functionalized Substrate

Elisabetta Canetta, Anne Leyrat, Claude Verdier

A physical model for studying adhesion between a living cell and a spherical functionalised substrate

E. Canetta, A. Leyrat and C. Verdier*

September 18, 2008

Laboratoire de Rhéologie[1], B.P. 53

Domaine Universitaire, 38041 Grenoble cedex 9, France

Abstract

A new microadhesion experiment is analysed in the framework of a stochastic model. Particular attention is focused on the adhesion between a functionalised spherical microsphere and a cell grown on a substrate. The parameters governing the dynamics of failure are deduced from the theory and the geometry of the system.

Keywords : Adhesion, Binding kinetics, Rupture force, Multiple bonds.

1 INTRODUCTION

Cellular adhesion is present in many aspects of cells life. Indeed, it is involved in a number of biological phenomena, such as the embryological development, the immune response and metastasis (development of secondary tumors) [1].

One of the aims of biophysical studies dealing with cellular adhesion, is to investigate the forces between bonds (i.e., receptor-ligand) [2, 3]. Indeed, adhesion is not only controlled by the nature and intensity of forces, as well as by the kinetics of formation and dissociation of bonds, but also by the ability of proteins to move along the cell membrane to form clusters or focal adhesion points. This knowledge should allow one to understand the mechanisms involved in cellular adhesion during processes of interest in the medical field, like in cancer metastasis (rolling, adhesion, spreading and transmigration). This should also help to identify targets for new therapies.

*claude.verdier@ujf-grenoble.fr

[1] Universités de Grenoble (UJF-INPG) and CNRS (UMR5520)

In this work, a new microadhesion experiment is proposed, coupled with microscopic techniques, in order to understand the adhesion between a cell and a spherical substrate (functionalised microsphere). In this context, a theoretical analysis is presented in the framework of the Evans and Ritchie's model of bond strength [4].

In section 2, the main interactions playing a fundamental role in cell-cell and cell-substrate adhesion are described. Section 3 is devoted to a description of the microadhesion experiment. In section 4, the Evans and Ritchie' model is illustrated. In section 5, the main results of the relationships between theoretical and experimental parameters in the cell-microsphere geometry case are presented. Finally, Section 6 deals with the relationships between theoretical and experimental parameters in the cell-microsphere geometry case.

2 CELLULAR ADHESION

Cell-cell and cell-substrate adhesion may be interpreted as a dynamic process mediated by specific weak[2] non-covalent interactions between complementary adhesion molecules (receptors and ligands) [2, 3].

Specific interactions are determined by the local geometry of receptors and ligands anchored either to the membranes of two cells (cell-cell adhesion), or to the cell membrane and the substrate (cell-substrate adhesion). These short-range ($\sim 1 - 2nm$) forces are the so-called "lock-and-key" interactions, because they arise when the ligand (*key*) fits into its complementary receptor (*lock*), thus creating a "binding pocket".

The interaction between a receptor and its ligand is also influenced by non-specific forces operating outside the binding pocket between the ligand surface and the cell membrane. Examples of such interactions are the electrostatic double-layer force, the van der Waals force and the steric repulsion. The superposition of the nonspecific forces and the specific interactions governs cellular adhesion by modifying the binding kinetics and the distribution of receptor-ligand bonds at equilibrium [3]. The analysis of the net interaction energy profile as a function of the separation distance between adhesion molecules, allows both to identify the different interactions governing the binding behaviour and to study the dissociation rates of receptor-ligand bonds.

3 EXPERIMENTAL METHODS

In order to investigate the adhesion dynamics of a cell-substrate system, we are developing a microadhesion experiment. We will use cells (for example endothelial cells), grown on a substrate, and study their interactions with a microsphere coated with adhesion proteins or components of the extracellular matrix (ECM), like collagen, fibronectin, laminin, etc.

[2] Biological adhesion is governed by weak interactions, because they allow dynamical processes (e.g., cell motility) which are at the basis of life.

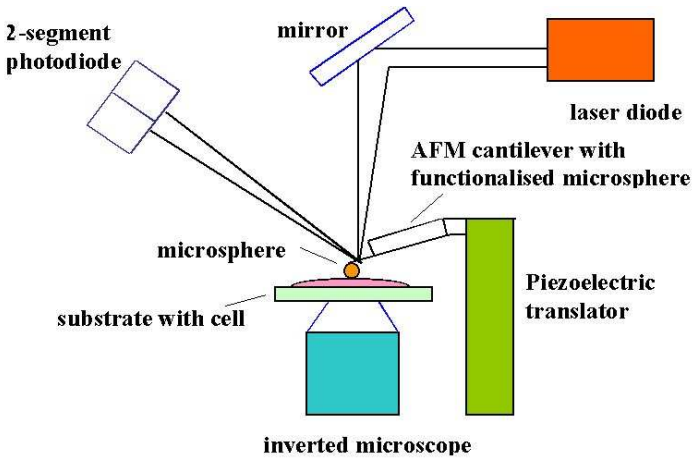

Figure 1: Experimental setup of the dynamic separation test.

The microadhesion test is performed on an inverted microscope equipped with Reflection Interference Contrast Microscopy [5] (for precise measurements of the system geometry) and with a home-built force spectrometer (based on AFM technology [6], Fig.1) which allows to measure interaction forces between the microsphere and the cells. Two complementary experiments are performed with this system : The JKR [7] test and the dynamic separation test.

3.1 JKR test

This test is based upon cell indentation by the microsphere, which is initially in contact with the cell (Fig.2). The purpose of the JKR method is to measure the force f, exerted by the microsphere of radius R onto the cell, and the radius a_{cm} of the contact zone (cf. 3.3) in order to determine the curve $a_{cm}(f)$, from which the local adhesion energy γ and elastic component K of the cell can be derived, using the following relation:

$$a_{cm}^3 = \frac{R}{K}\left(f + 3\pi R\gamma + \sqrt{6\pi R\gamma f + (3\pi R\gamma)^2}\right), \tag{1}$$

where K is given by,

$$K = \frac{4E}{3\left(1-\nu^2\right)}, \tag{2}$$

In Eq.(2), ν is the Poisson ratio and E is the local Young modulus of the cell, which is considered to be purely elastic at this scale.

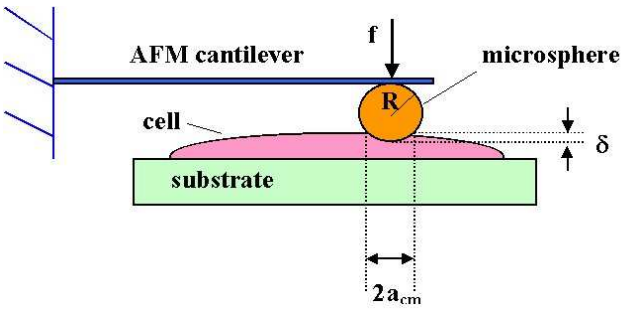

Figure 2: Sketch of the JKR technique for interaction between a cell and a functionalised microsphere. The contact diameter $2a$ is a function of the microsphere radius R, the surface energy γ and the local elastic component of the cell K (Eq.(1)). δ is the indentation and f is the applied force.

3.2 Dynamic separation test

In this test, the microsphere is pulled vertically at a given velocity, while recording the force signal. This corresponds to measuring the complex deformation of the cell (force rise) until bonds start to break (decrease in force) as they would in a micropeel test. Knowing the elastic constant of the cantilever k_f, its deflection allows to determine the force $f(t)$ exerted by the microsphere on the cell, which is a function of the observation time t. By means of a careful analysis of this force signal (Sec.5), the bond strength f^* may be deduced, as well as the lifetime Δt of the area of bonding.

3.3 Materials and methods

Microscopic observations: In order to localise and visualise the cells, this apparatus is mounted on the Zeiss Axiovert 200 inverted microscope, equipped with a Neofluar 63/1.25 Antiflex objective, which allows to perform RICM (Reflection Interference Contrast Microscopy) and fluorescence observations. RICM is a microscopic technique used to measure the radius and the angle of the contact zone between the cell and the substrate (Fig.3a). It can also be employed to determine the geometry of the cell-microsphere interface (Fig.3b), in order to find the peeling velocity v_p of the contact area of the cell-microsphere system (Sec.6). In Fig.3a (3b), the RICM principle is illustrated for the cell-substrate (microsphere) case. The incident beam I_0 is partly reflected by the substrate (cell)-medium interface (beam I_1). The transmitted part is reflected by the cell (microsphere) with an intensity I_2. The RICM image is formed by the interference of the beams (I_1 and I_2) when imaged in the microscope objective. The analysis of this image allows to obtain the radius a_{cc} (a_{cm}) and the angle θ_{cc}

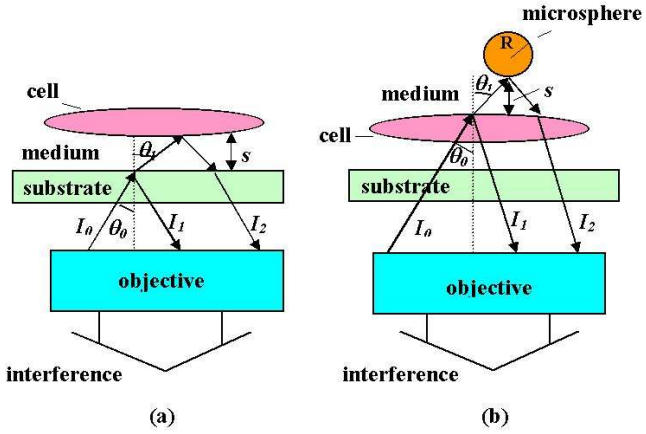

Figure 3: The basic principle of RICM. (a) Cell-substrate case: The cell is observed under epi-illumination using monochromatic light, I_0 ($\lambda = 546.1nm$). Interference fringes arise from the difference in the optical path of light reflected from the substrate-medium interface I_1 and from the cell-medium interface I_2. s is the vertical separation between the cell and substrate ($s = 0 \rightarrow$ contact). θ_0 is the incident angle and θ_1 is the angle of refraction in the medium (Snell's law). (b) Same as (a) but in the cell-microsphere case.

(θ_{cm}) of the cell-substrate (microsphere) contact zone (Fig.4) [5]. Fluorescence observations will be helpful in order to localize and to identify fluorescently labelled adhesion molecules.

Force measurements: The force measurements are performed using a functionalised microsphere which is glued onto a soft AFM cantilever (Veeco Instruments, France), with nominal spring constant $k_f = 0.06N/m$. The microsphere is positioned relatively to the cell by means of a vertical piezo translator with a capacitive position sensor (Trioptics, France). When the cell exerts a force on the microsphere (for instance, when the microsphere is retracted from the cell in the dynamic separation test), the AFM cantilever undergoes a deflection which is measured by means of a laser spot reflected off the back of the cantilever onto a two-segment photodiode (Optoprim, France). To sum up, the combination of these techniques allows to obtain nine parameters: The radius a_{cc} (a_{cm}), the angle θ_{cc} (θ_{cm}) of the cell-substrate (microsphere) contact area, the bond strength f^*, the lifetime Δt of the area of bonding, the peeling velocity v_p, the local adhesion energy γ and elastic component K of the cell.

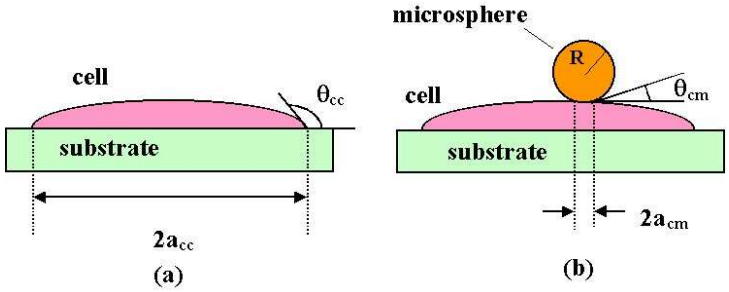

Figure 4: (a) The radius a_{cc} and the angle θ_{cc} of the cell-substrate contact zone, measured by means of the RICM technique. (b) The contact radius a_{cm} and the contact angle θ_{cm} in the cell-microsphere case.

4 THE MODEL OF EVANS AND RITCHIE

We have analysed the experimental parameters described in Sec.3, in the framework of the stochastic model of induced bond failure developed by Evans and Ritchie [4]. They model a receptor-ligand bond as confinement by a single activation energy E_b of the energy landscape $E(x)$. The application of a force f produces a mechanical potential, thus tilting the energy landscape $E(x)$ and lowering the activation energy E_b (Fig.5). By using the Kramer's rate theory [8], Evans and Ritchie obtained an expression for the *kinetic rate* $K_r(f)$ of the dissociation of a *single* bond[3], which depends exponentially on the applied force f [4]:

$$K_r(f) \approx \left(\frac{1}{t_{OFF}}\right) \cdot g\left(\frac{f}{f_\beta}\right) \cdot exp\left(\frac{f}{f_\beta}\right). \tag{3}$$

In Eq.(3), $g\left(\frac{f}{f_\beta}\right)$ [4] is a weak force-dependent factor taking into account the displacement and the change of barrier width caused by an applied force. f_β is the characteristic force scale given by the ratio of thermal energy k_BT to the distance x_β of the activation barrier along the direction of force ($f_\beta = \frac{k_BT}{x_\beta}$). Finally, $\frac{1}{t_{OFF}}$ is the spontaneous (zero-force) rate of dissociation depending on the energy barrier E_b [4],

$$\frac{1}{t_{OFF}} = \frac{1}{t_D} \cdot exp\left(-\frac{E_b}{k_BT}\right), \tag{4}$$

[3] The energy landscape of a single bond is constituted by a single activation barrier.

[4] For single bonding potentials, $g\left(\frac{f}{f_\beta}\right) \sim \left(\frac{f}{f_\beta}\right)^a$, where $\frac{1}{2} < a < 1$. In particular, $a \approx \frac{1}{2}$ for inverse power law attraction and $a \approx 1$ for deep harmonic well [4].

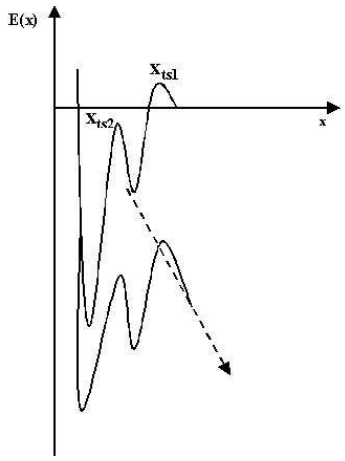

Figure 5: A cascade of barriers under force where an inner barrier emerges to dominate kinetics when the outer barrier falls below by $\sim k_B T$. $x_{tsi}\,(i = 1, 2)$ represents the transitions states to the unbound state (graph replotted from Ref.[12]).

where t_D is a characteristic time constant for diffusive escape. According to the Evans and Ritchie model, bond dissociation is treated as a first-order Markov process with increasing rate of dissociation driven by the rising force. The result is a statistical distribution of forces of rupture whose maximum defines the *single-bond strength* f^* which increases with the load applied to a bond. In particular, f^* is related to the loading rate (force/time) r_f, by means of the following expression [9]:

$$\frac{1}{r_f} = \frac{t_{OFF}}{f_\beta} \cdot exp\left(-\frac{f^*}{f_\beta}\right). \tag{5}$$

In the case of a complex bond[5], where one has a hierarchy of activation barriers, the spectrum of bond strength will be constituted by a sequence of linear regimes with ascending slopes f_β [10]. Each *n-th* activation barrier in the hierarchy is described by a spontaneous rate of dissociation $\frac{1}{t_{OFF}}$ and a force scale $f_\beta\,(n) = \frac{k_B T}{x_\beta(n)}$. The fact that the slope $f_\beta\,(n)$ increases from one linear regime to the next, means that activation barriers emerge in succession from outer to inner positions, along the direction of applied force, to dominate kinetics. The determination of bond strength f^* becomes most complicated when N single (or complex) bonds occur. Three different mechanical scenarios for these multiple bonds can be considered: Series, zipper [10, 11] and parallel [10]. When N bonds are in series, each of them fully experiences the applied force, but can break either cooperatively or uncooperatively. In the first case,

[5] Unlike a single bond, where one only needs to traverse an activation barrier to break it, the rupture of a complex bond involves the crossing of a cascade of activation barriers.

the bonds behave as a macro-single bond whose barrier energy is given by the sum of barrier energies of each bond. On the contrary, when the N bonds fail in an uncooperative way, each of them experiences the same force history and when any bond breaks, the attachement as a whole fails. In the zipper model [10, 11], the N bonds fail in sequence in a random way from first to last. This means that once a bond fails, force propagates to the next one, and so on. Finally, in the case of bonds in parallel, the applied force is partitioned among receptor-ligand bonds which form the adhesion between the cell and the substrate (or another cell). In particular, when identical bonds are loaded in parallel, the applied force f is shared equally by each bond.

5 RELATIONSHIP BETWEEN THE ADHESION FORCE AND THE SEPARATION VELOCITY

In the analysis of the physical parameters obtained from the experiment, we focus our attention on the relationship between the most frequent rupture force f^* and the separation velocity v_s of the microsphere. We study the case of the occurrence of N receptor-ligand bonds, assuming the N bonds in parallel, which seems more realistic [10]. We suppose that the cell and the functionalised microsphere adhere to each other by means of N weak identical bonds held by rigid linkages. This hypothesis simplifies the computation, because it does not consider any flexible polymer chain [12]. We also assume that the N bonds are loaded in parallel and that each of them is a single bond (one activation barrier in the energy landscape). As stated in the previous section, N identical bonds loaded in parallel experience the same quantity of the applied force f. With this rule in mind, and starting from the probability density for bond rupture [13], we obtaine the following general expression for the most frequent rupture force f^*

$$f^* \approx N f_\beta \cdot ln\left(\frac{t_{OFF} \cdot r_f}{\left(\frac{f^*}{N f_\beta}\right)^a \cdot \left(\frac{f^*}{a}\right)}\right). \tag{6}$$

As expected [10], the expression (6) is a transcendental equation where t_{OFF} is the time needed to detach the cell from the microsphere when no external force is applied (Eq.(2)), r_f is the loading rate, a is a constant ranging from $\frac{1}{2}$ to 1 according to the bonding potential considered (see footnote 5 on page 4), and f_β is the thermal force scale. By analysing the relationship between the spontaneous rate $\frac{1}{t_{OFF}}$ and the kinetic rate $K_r\left(\frac{f}{N}\right)$ of dissociation of a single bond (Eq.(3)), from Eq.(6) we can get the dissociation rate as a function of the most frequent rupture force f^* (when $f^* << N f_\beta$):

$$K_r\left(\frac{f^*}{N}\right) \approx a \cdot r_f \cdot \left(\frac{1}{f^*} + \frac{1}{N f_\beta}\right) \cdot exp\left(-\frac{f^*}{N f_\beta}\right). \tag{7}$$

The separation velocity v_s, of the functionalised microsphere from the cell, can be calculated by [13],

$$v_s = \Delta Z \cdot K_r \left(\frac{f^*}{N} \right). \tag{8}$$

In Eq.(8), $Z = \xi - \left(\frac{f^*}{k_f} \right)$ is the time dependent reaction coordinate describing the rupture process of the cell-microsphere system. ξ is the cantilever displacement and $\frac{f^*}{k_f}$ is the ratio of most probable rupture force f^* to the spring constant k_f of the AFM cantilever to which the microsphere is attached (Fig.1). $\frac{f^*}{k_f}$ is the deflection undergone by the cantilever when the microsphere is retracted from the cell. ΔZ is the difference between two such coordinates evaluated at the time of detachment and the beginning of peeling, respectively. By substituting Eq.(7) in Eq.(8), it is immediate to obtain the rupture force f^* as a function of the separation velocity v_s:

$$f^* \approx N \cdot f_\beta \cdot ln \left[\frac{a \cdot \Delta Z \cdot r_f}{v_s N f_\beta} \cdot \left(\frac{N f_\beta}{f^*} + 1 \right) \right]. \tag{9}$$

Eq.(9) shows that the most probable rupture force f^* increases linearly with the logarithm of the pulling velocity v_s, as expected [10]. In particular, Eq.(9) allows us to obtain a thermal scale for force $N f_\beta$ and hence to map the energy barrier to a distance x_β, along the direction of force, to the ground state (i.e., $x_\beta = \frac{k_B T}{N f_\beta}$). This mapping provides us informations about the location of transition states to the unbound state [10].

6 APPLICATION TO THE CELL-MICROSPHERE ZONE

In order to improve the theoretical knowledge of the cell-microsphere interactions, we study the contact zone between the cell and the microsphere. This will allow to analyse the experimental parameters from the dynamic separation technique (see Sec.3). In particular, the relationship existing between the peeling velocity v_p of the contact area and the adhesion force f^* will be derived. Simplified results about the relationship between the peeling velocity v_p and the speed of separation v_s will be also obtained.

In Fig.6, the geometry of the cell-microsphere contact zone at two subsequent times t and t' is shown. A local approach is used, where only the important part of the cell is considered. At time t, the microsphere has just been made to adhere to the cell and after a time interval $\Delta t = t' - t$, it has moved up by a distance $h = S' - S$, where S and S' are the distances between the microsphere and the substrate at the time t and t', respectively (Fig.6). From a geometrical

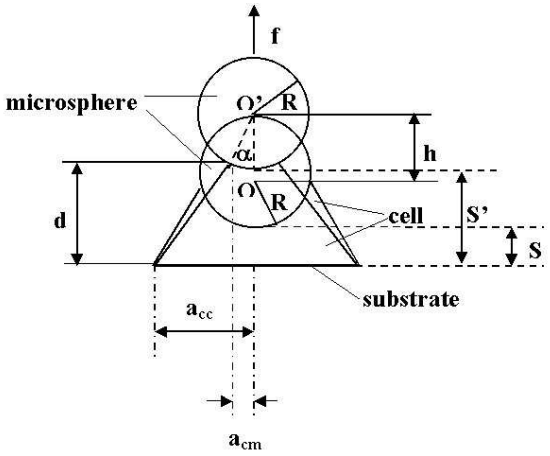

Figure 6: Sketch of the local geometry of the contact area between the cell and the microsphere of radius R, at two subsequent times, t and t', when the microsphere is pulled away from the cell with an applied force f.

point of view, the peeling velocity v_p is the time derivative of the contact arc between the cell and the microsphere, and can be written as:

$$v_p = v_s \frac{2\pi R A^2}{\pi \left(a'_{cm} \left[2R^2 - A^2 - 3\left(a'_{cm}\right)^2 \right] - \rho d' \left[a_{cc} + 2a'_{cm} \right] \right) + 4R^3}. \qquad (10)$$

In Eq.(10), $A^2 = a_{cc}^2 + a_{cc} \cdot a'_{cm} + \left(a'_{cm}\right)^2$ where a_{cc} and a'_{cm} are the radii of the cell-substrate contact zone at time t and the cell-microsphere contant zone at time t' (Fig.6), respectively. $\rho = \sqrt{R^2 - \left(a'_{cm}\right)^2}$, with R the radius of the microsphere, and d' is defined in Fig.6. This result shows that when a'_{cm} is quite small (presumably at the end of peel), then v_p will be positive only if $h' < \frac{4R^2}{\pi a_{cc}}$. This result is to be compared with a similar one obtained by Shanahan [14], dealing with adhesion of a punch to a thin membrane, when assuming a weak surface energy. In such cases, peeling is not possible due to the geometry. To summarize, Eq.(10) gives the final relationship allowing to predict the peeling velocity in order to get $f^*(v_p)$ curves.

7 CONCLUSIONS

The parameters obtained from a new microadhesion experiment have been analysed both in the framework of a stochastic model, and also experimentally. By using the Evans and Ritchie's model of bond strength [4], we found a simple relationship between the most probable rupture force f^* and the separation

velocity v_s of the contact zone between a cell and a microsphere, in the case of N identical bonds in parallel, held by rigid linkages. As expected [10], the adhesion force f^* depends linearly on the logarithm of the separation velocity, and the slope provides us information about the location of transition states to the unbound state. Finally, the microadhesion test is shown to be able to provide all the parameters required in the model.

AKNOWLEDGEMENTS

This work was supported by the RTN project funded by the EU, contract n° CT-2000-00105.

References

[1] I. Saiki, Cell adhesion molecules and cancer metastasis, *Jpn. J. Pharmacol.* **75**, 215-242 (1997).

[2] J. Israelachvili, *Intermolecular and surface forces*, Academic Press, London (1985).

[3] D. Leckband, Measuring the forces that control protein interactions, *Annu. Rev. Biophys. Biomol. Struct.* **29**, 1-26 (2000).

[4] E. Evans and K. Ritchie, Dynamic strength of molecular adhesion bonds, *Biophys. J.* **72**, 1541-1555 (1997).

[5] J.O. Rädler, T.J. Feder, H.H. Strey and E. Sackmann, Fluctuation analysis of tension-controlled modulation forces between giant vesicles and solid substrates, *Phys. Rev. E* **51**, 4526-4536 (1995).

[6] G. Binning, C.F. Quate and C. Gerber, Atomic force microscope, *Phys. Rev. Lett.* **56**, 930-933 (1986).

[7] K.L. Johnson, K. Kendall and A.D. Roberts, Surface energy and the contact of elastic solids, *Proc. R. Soc. Lond. A.* **324**, 301-313 (1971).

[8] H.A. Kramers, Brownian motion in a field of force and the diffusion model of chemical reactions, *Physica* **7**, 284-304 (1940).

[9] E. Evans, A. Leung, D. Hammer and S. Simon, Chemically distinct transition states govern rapid dissociation of single L-selectin bonds under force, *Proc. Natl. Acad. Sci. USA* **98** (7), 3784-3789 (2001).

[10] E. Evans, Probing the relation between force-lifetime-and chemistry molecular bonds, *Annu. Rev. Biophys. Biomol. Struct.* **30**, 105-128 (2001).

[11] T. Strunz, K. Oroszlan, I. Schumakovitch, H.J. Güntherodt and M. Hegher, Model energy landscapes and the force-induced dissociation of ligand-receptor bonds, *Biophys. J.* **79**, 1206-1212 (2000).

[12] E.Evans and K. Ritchie, Strength of a weak bond connecting flexible polymer chains, *Biophys. J.* **76**, 2439-2447 (1999).

[13] B. Heymann and H. Grubmüller, Dynamic force spectroscopy of molecular adhesion bonds, *Phys. Rev. Lett.* **84** (26), 6126-6129 (2000).

[14] M.E.R. Shanahan, Adhesion of a punch to a thin membrane, *C.R. Acad. Sci. Paris* **IV** (1), 517-522 (2000).